Force Actuator based Articulated Suspension Vehicle for Rough Terrain Mobility

Vijay P. Eathakota, Srikanth Kolachalama, Arun K. Singh and K. Madhava Krishna

Abstract— **In this paper we developed a model of a Linear Force Actuator based actively articulated suspension vehicle (LFA-V) with toroidal wheels and proposed a strategy to control its contact forces to improve traction on an uneven terrain. We developed the quasi-static analysis for our vehicle and compared the maneuverability of our vehicle with that of a passive suspension system. Extensive uneven terrain simulations depict the efficacy of our proposed system.**

I. INTRODUCTION

To improve the mobility of wheeled robots traversing on an uneven terrain having slopes in all three orthogonal directions is the primary focus of our research. Past research on 'all terrain vehicles', [1],[2] was focused on developing mechanical suspension systems which could improve terrain adaptability and locomotion. Consequently control algorithms were developed for posture stability of the vehicle [3], [4]. Shrimp robots [1] and Rocky rovers [2] are terrain vehicles with passive suspension systems which have excellent terrain adaptability and ability to negotiate terrains having discontinuities that are higher than the wheel radius but the mobility of such vehicles is not guaranteed. Thus for such conditions Sreenivasan and Waldron [4] developed vehicles called Wheeled and Actively Articulated Vehicles (WAAVs). CH. Grand *et al* [5], [8] developed another type of such vehicle called Hybrid Wheel Legged vehicle (Hylos). Posture control algorithm for Hylos was developed by mapping the velocities at various joints to the velocity of the main body based on posture error which improves traction and stability. K. Iagnemma and S. Dubowsky [6] developed a traction control algorithm to improve ground traction of a vehicle traversing on rough terrain while optimizing power consumption. Hence we proposed LFA-V to improve traction. We also introduced a method for calculating the traction force at each wheel and presented the Quasi Static Analysis for the system. The depiction of the enhanced feasibility regions of LFA-V compared with that of passive suspension vehicle confirm the efficacy of the proposed method. Simulations results are also reported for measurements corrupted by additive Gaussian noise with its mean shifted up to 15% of the actual value.

Vijay Eathakota, Srikanth Kolachalama Arun K. Singh and K. Madhava Krishna are with the Robotics Research Centre, International Institute of Information Technology, Hyderabad, India. (vijay@research.iiit.ac.in, srimech2004@gmail.com, aks1812@gmail.com and mkrishna@iiit.ac.in).

II. ANALYSIS OF PASSIVE SUSPENSION SYSTEM

We analyzed a passive suspension vehicle on an uneven terrain and introduced our motivation to develop LFA-V.

Let ψ, ro and yo be the pitch, roll and yaw angles respectively of the chassis about the global $\{XYZ\}$ axes respectively. The resultant rotation matrix relating position vectors with respect to global reference frame is given by [7]

$$R = R_z(yo).R_y(ro).R_x(\psi) \quad (1)$$

Where $R_x(\psi)$, $R_y(ro)$ and $R_z(yo)$ are the rotation matrices corresponding to the Euler angles about the X, Y and Z axes respectively. In a passive suspension system two forces act at the point of contact of i^{th} wheel.

i) The normal force $\overline{N}_i = \begin{bmatrix} N_{xi} & N_{yi} & N_{zi} \end{bmatrix}^T$

ii) The traction force $\overline{T}_i = \begin{bmatrix} T_{xi} & T_{yi} & T_{zi} \end{bmatrix}^T$

Since the motion of our vehicle is in the YZ plane, there is no loss of generality in assuming $T_{xi} \approx 0$ and $T_{yi} > 0$. (2)

Under no slip conditions we have

$$\left|\overline{T}_i\right| \le \mu_i \left|\overline{N}_i\right| \quad \forall \quad i \in \{1,2,3,4\} \quad (3)$$

Where μ_i is the coefficient of friction between the point of contact of i^{th} wheel and the terrain.

Since $\overline{T}_i$ is always perpendicular to $\overline{N}_i$ we have

$$dot(\overline{T}_i, \overline{N}_i) = 0 \implies N_{xi}T_{xi} + N_{yi}T_{yi} + N_{zi}T_{zi} = 0 \quad (4)$$

From (2) the maximum magnitude of $\left|\overline{T}_i\right|$ under no slip condition is $\mu_i\left|\overline{N}_i\right|$. *i.e*

$$\left|\overline{T}_i\right| = \mu_i\left|\overline{N}_i\right| \implies T_{xi}^2 + T_{yi}^2 + T_{zi}^2 = \mu_i^2 N_i^2 \quad (5)$$

Case 1: If $\left|\overline{N}_i\right| = 0$ then $\left|\overline{T}_i\right| = 0$. Since the wheel will lose contact from the surface of the terrain.

Case 2: If $\left|\overline{N}_i\right| \neq 0$ then any one of the components $N_{xi}, N_{yi}, N_{zi} \neq 0$, let $N_{zi} \neq 0$, then from (4) and (5) we get

$$\mu_i^2\left|\overline{N}_i^2\right| - T_{xi}^2 = T_{yi}^2 + \left[\frac{N_{xi}T_{xi} + N_{yi}T_{yi}}{N_{zi}}\right]^2 \quad (6)$$

$$(6) \implies aT_{yi}^2 + bT_{yi} + c = 0 \quad (7)$$

Where $a = (N_{zi}^2 + N_{yi}^2)$, $b = 2.N_{xi}T_{xi}N_{yi}$

$c = T_{xi}^2(N_{zi}^2 + N_{xi}^2) - \mu_i^2 \left|\overline{N}_i\right|^2 N_{zi}^2$.

Since $a \neq 0$ equation (7) is quadratic in nature and will have real roots if $b^2 - 4ac \geq 0 \Leftrightarrow \dfrac{\mu_i \left|\overline{N}_i\right|}{\left|N_{zi}\right|} \geq T_{xi}$ which is always true by (2). Therefore we get

$$T_{yi} = \frac{\mu_i \left|\overline{N}_i\right| \left|N_{zi}\right|}{\sqrt{N_{zi}^2 + N_{yi}^2}} \quad \text{and} \quad T_{zi} = \frac{-\mu_i N_{yi} \left|\overline{N}_i\right| \left|N_{zi}\right|}{N_{zi}\sqrt{N_{zi}^2 + N_{yi}^2}} \qquad (8)$$

Let the unit vectors of $\overline{T}_i$ and $\overline{N}_i$ be

$$\hat{t}_i = \frac{\overline{T}_i}{\left|\overline{T}_i\right|} = [t_{xi}\ t_{yi}\ t_{zi}]^T \text{ and } \hat{n}_i = \frac{\overline{N}_i}{\left|\overline{N}_i\right|} = [n_{xi}\ n_{yi}\ n_{zi}]^T$$

Assumption: 1 Quasi-static analysis is done on the system assuming the masses of legs and wheels are negligible when compared to the mass of the chassis. Now the net force acting and net moment acting on the system is given by

$$\overline{F} = \left[F_x\ F_y\ F_z\right]^T = \sum_{i=1}^{4}(\overline{T}_i + \overline{N}_i) + M\overline{g}. \qquad (9)$$

$$\overline{M} = \sum_{i=1}^{4}[\overline{r}_{tni} \times (\overline{T}_i + \overline{N}_i)] = \left[M_x\ M_y\ M_z\right]^T. \qquad (10)$$

Where $F_x = 0$, $F_z = Mg$, M is the mass of the chassis, g is the acceleration due to gravity, F_y is the force which we command to drive the system and $\overline{r}_{tni}$ is the radius vector from the CG to the point of contact of the i^{th} wheel.

$\overline{r}_{tni} = \overline{r}_{fai} + \overline{r}_1 + \overline{r}_2 + \overline{r}_3$ where

$$\overline{r}_{fai} = \left\{ R.\left[\frac{(2.5-i)}{|2.5-i|} w \quad (-1)^{i+1} a \quad 0\right]^T \right. \quad \forall\ i \in \{1,2,3,4\}$$

$2a \Rightarrow$ Length of the chassis, $2w \Rightarrow$ Width of the chassis

$\overline{r}_1 = R.[0\ 0\ -l_i]^T$

$\overline{r}_2 = R.[0\ -r\sin(\gamma_i)\ -r\cos(\gamma_i)]^T, \gamma_i \approx \arctan\left(N_{yi} / N_{zi}\right)$

$\overline{r}_3 = -r_t.\hat{n}_i$.

Where l_i is the length of the i^{th} leg, r is the radius of the wheels, r_t is the radius of the torodial cross section. We obtain $\overline{N}_i, l_i, \psi, ro$ and yo from MSC Visual Nastran. Let $[m_{txi}\ m_{tyi}\ m_{tzi}\ ]^T$, $[m_{nxi}\ m_{nyi}\ m_{nzi}\ ]^T$ be the unit moment vectors due to $\overline{T}_i$ and $\overline{N}_i$ respectively.

Now let $AC = D$ (11)

Where

$C = [\left|\overline{T}_1\right|\ \left|\overline{N}_1\right|\ \left|\overline{T}_2\right|\ \left|\overline{N}_2\right|\ \left|\overline{T}_3\right|\ \left|\overline{N}_3\right|\ \left|\overline{T}_4\right|\ \left|\overline{N}_4\right|]^T$

$D = [F_x\ F_y\ F_z\ M_x\ M_y\ M_z]^T$ and

$$A = \begin{bmatrix} t_{x1} & n_{x1} & t_{x2} & n_{x2} & t_{x3} & n_{x3} & t_{x4} & n_{x4} \\ t_{y1} & n_{y1} & t_{y2} & n_{y2} & t_{y3} & n_{y4} & t_{y4} & n_{y4} \\ t_{z1} & n_{z1} & t_{z2} & n_{z2} & t_{z3} & n_{z3} & t_{z4} & n_{z4} \\ m_{tx1} & m_{nx1} & m_{tx2} & m_{nx2} & m_{tx3} & m_{nx3} & m_{tx4} & m_{nx4} \\ m_{ty1} & m_{ny1} & m_{ty2} & m_{ny2} & m_{ty3} & m_{ny3} & m_{ty4} & m_{ny4} \\ m_{tz1} & m_{nz1} & m_{tz2} & m_{nz2} & m_{tz3} & m_{nz3} & m_{tz4} & m_{nz4} \end{bmatrix}$$

Equation (11) are has infinite set of solutions for C. Now let

$$\min(S), S = \sum_{i=1}^{4}\left|\overline{T}_i\right|. \qquad (12)$$

$$\left|\overline{N}_i\right| \geq 0 \quad \forall\ i = \{1,2,3,4\} \qquad (13)$$

$$\Gamma_i^{\min} \leq (\left|\overline{T}_i\right|.r) \leq \Gamma_i^{\max} \quad \forall\ i = \{1,2,3,4\} \qquad (14)$$

$\Gamma_i^{\max}, \Gamma_i^{\min}$ are the maximum and minimum torques that the motor at the i^{th} wheel can generate. For the vehicle to move forward and remain in equilibrium we set $F_Y > 0$, and $\left|\overline{M}\right| = 0$. To depict the regions of infeasibility we solve an arbitrary optimization problem (12) subject to the equality constraint (11) and a set of inequality constraints given by (3), (13) and (14).For the simplicity of analysis we assume the front wheels are at contact angle γ_1 and rear wheels are at contact angle γ_2 which are varied from 0 to $\pi/2$ and ψ is varied from 0 to $(\gamma_1 - \gamma_2)$.

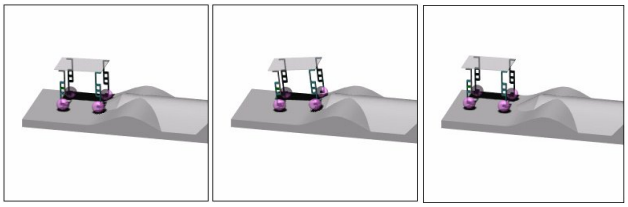

Fig. 1 A passive suspension Vehicle unable to negotiate an uneven terrain as it gets pushed back upon reaching a slope

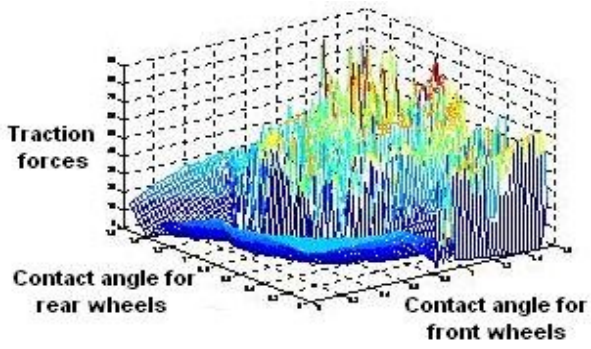

Fig.2.Plot of min(T_1+ T_2 +T_3+ T_4) Vs contact angles showing regions of infeasibility (discontinuous surface)

Fig. 2 shows the plot of $\min(\sum_{i=1}^{4}|\overline{T}_i|)$ as a function of the contact angles γ_1, γ_2 .The discontinuities in the plot depict the regions of infeasibility to (12).

III. Analysis of LFA-V

For controlling the contact forces and to ensure a permanent contact condition, we developed an actively articulated suspension system and exploited its internal degree of mobility by an actuated prismatic joint through a linear force actuator mounted on the chassis. We use a generic platform consisting of a chassis, prismatic joints and four toroidal wheels each pinned to an outer slide link of a prismatic joint, where as the inner slide link was fixed to the chassis as shown in Fig 3. In LFA-V three forces act at the i^{th} wheel. They are $\overline{N}_i$, $\overline{T}_i$ and the actuator force $\overline{F}_i^A$ .Now a similar analysis is done for LFA-V.

$\overline{F}_i^A$ is always perpendicular to the chassis *i.e*

$$\overline{F}_i^A = \frac{|\overline{N}_i|}{dot(\hat{n}_i, \hat{f}_i^A)}\hat{f}_i^A \quad \text{.Where} \quad \hat{f}_i^A = R.[0 \;\; 0 \;\; 1]^T \qquad (15)$$

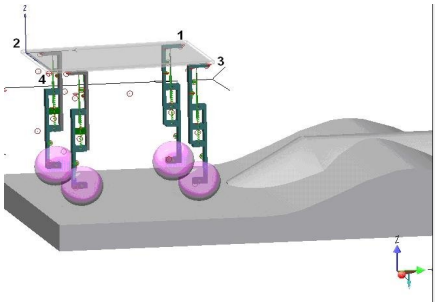

Fig.3 LFA-V

Remark: Along the sliding direction the only force to be considered is the commanded $\overline{F}_i^A$. Assuming the suspension system of LFA-V to be an ideal suspension system, the property of a prismatic joint with linear force actuator is that only the components of $\overline{T}_i$ and $\overline{N}_i$ perpendicular to $\overline{F}_i^A$ get transmitted to the chassis. To find the components of $\overline{T}_i$ perpendicular to $\overline{F}_i^A$, we find $\overline{R}_{tai}$ which is resulted when $\hat{f}_i^A$ is rotated by $\frac{\pi}{2}$ radians towards $\hat{t}_i$ about $\overline{K}_{ti} = cross(\hat{t}_i, \hat{f}_i^A)$ [7].

$$\overline{R}_{tai} = R_{K_{ti}}(\frac{\pi}{2})\hat{f}_i^A. \qquad (16)$$

Where $\frac{\overline{K}_{ti}}{|\overline{K}_{ti}|} = [k_{txi} \;\; k_{tyi} \;\; k_{tzi}]^T$ and

$$R_{K_{ti}}(\frac{\pi}{2}) = \begin{bmatrix} k_{txi}^2 & k_{txi}k_{tyi} - k_{tzi} & k_{txi}k_{tzi} + k_{tyi} \\ k_{txi}k_{tyi} + k_{tzi} & k_{tyi}^2 & k_{tyi}k_{tzi} - k_{txi} \\ k_{txi}k_{tzi} - k_{tyi} & k_{tyi}k_{tzi} + k_{txi} & k_{tzi}^2 \end{bmatrix} \qquad (17)$$

Hence the component $\overline{T}_i$ perpendicular to $\overline{F}_i^A$ is given by

$$\overline{T}_{neti} = dot(\hat{t}_i, \overline{R}_{tai})|\overline{T}_i|.\overline{R}_{tai}. \qquad (18)$$

Similarly component of $\overline{N}_i$ perpendicular to $\overline{F}_i^A$ is given by $\overline{N}_{neti} = dot(\hat{t}_i, \overline{R}_{nai})|\overline{N}_i|.\overline{R}_{nai}$. (19)

Let the unit vectors of $\overline{T}_{neti}$ and $\overline{N}_{neti}$ be

$$\hat{t}_{neti} = \frac{\overline{T}_{neti}}{|\overline{T}_{neti}|} = [t_{netxi} \; t_{netyi} \; t_{netzi}]^T \text{ and}$$

$$\hat{n}_{neti} = \frac{\overline{N}_{neti}}{|\overline{N}_{neti}|} = [n_{netxi} \; n_{netyi} \; n_{netzi}]^T$$

Hence the net force and the net moment acting on the chassis of the vehicle is given by

$$\overline{F} = \sum_{i=1}^{4}(\overline{F}_i^A + \overline{T}_{neti} + \overline{N}_{neti}) \qquad (20)$$

$$\overline{M} = \sum_{i=1}^{4}[(\overline{r}_{fai} \times \overline{F}_i^A) + \overline{r}_{tni} \times (\overline{T}_{neti} + \overline{N}_{neti})] \qquad (21)$$

Let $B.C = D$ (22)

Where B is a matrix of 6x8 dimension similar to A.

To attain a desired posture to the chassis, the vehicle parameters that need to be controlled while traversing a terrain are the height h of the chassis, velocity V in Y direction, ψ, ro and yo. Therefore we commanded a suitable value of $M_x = \overline{k}_p e_\psi + \overline{k}_v \dot{e}_\psi$, $M_y = \breve{k}_p e_{ro} + \breve{k}_v \dot{e}_{ro}$ and $M_z = \tilde{k}_p e_{yo} + \tilde{k}_v \dot{e}_{yo}$. Where $e_\psi = \psi_d - \psi$, $e_{ro} = ro_d - ro$ and $e_{yo} = yo_d - yo$. Similarly we have $F_y = \breve{k}_p e_v + \breve{k}_d \dot{e}_v$ and $F_z = k_p e_h + k_v \dot{e}_h + Mg$, where $e_v = V_d - V$ and $e_h = h_d - h$. e_v, e_h, e_ψ, e_{ro} and e_{yo} are the differences between desired and the instantaneous values of the parameters being controlled. $k_p, \overline{k}_p, \hat{k}_p, \tilde{k}_p, \breve{k}_p$ and $k_v, \overline{k}_v, \hat{k}_v, \tilde{k}_v, \breve{k}_v$ are the proportional and derivative gains respectively.

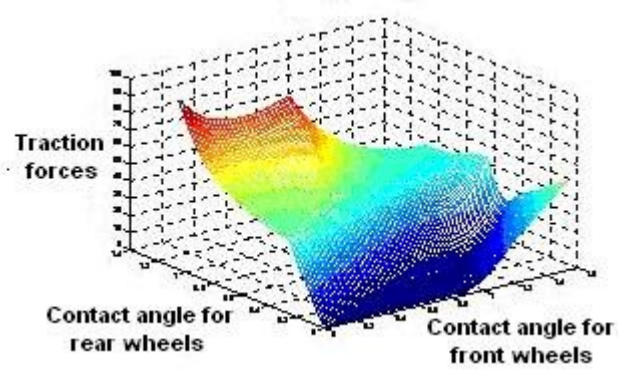

Fig. 4 Plot of min(T_1+ T_2 +T_3+ T_4) Vs contact angles showing regions of infeasibility

Control equations were developed to overcome the differences in the vehicle dynamics due to the assumption 1. Now to show that infeasibility regions are eliminated, similar analysis has been carried out by solving the optimization problem (12) with the inequality constraints (3),(13) ,(14) and equality constraint(22). From Fig. 4 it is easy to see that the infeasibility regions are completely eliminated for LFA-V.

IV. RESULTS AND DISCUSSION

Simulations were performed using MATLAB, Simulink and MSC Visual Nastran on terrains 1, 2 which were modeled such that every point on the surface has a finite and unique gradient in any three orthogonal directions as shown in Fig's 5-6. The controllers were applied to maintain V_d =0.5m/s, h_d =0.42m, $\psi_d = ro_d = yo_d = 0$ by assuming M =9.31 Kg, a =0.3m, w =0.2m, $r_t = 0.0125$m and r =0.05m. From the Fig.7 and Fig.8 we observe that the force actuator applies force ensuring sufficient traction and more importantly $\left|\overline{F}_i^A\right|$ is very high at steep slopes. Fig.9 and Fig.10 show the plots of Euler angles for the terrains 1 and 2. It is easy to see that the deviations of these angles were well within acceptable limits. Fig.11 and Fig.12 show the plots of velocities of LFA-V on terrains1, 2 where the desired velocity is maintained.

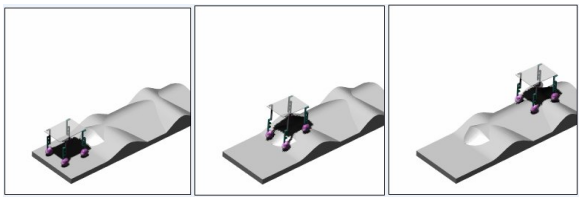

Fig. 5 LFA-V negotiating terrain -1

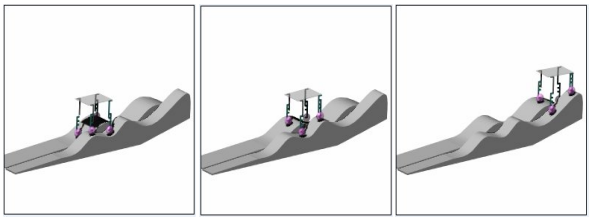

Fig. 6 LFA-V negotiating terrain-2.

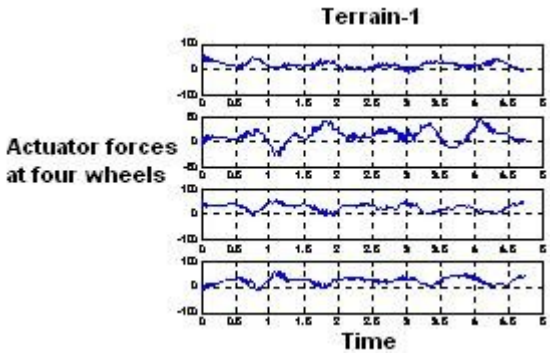

Fig. 7 The plot of actuator forces for terrain-1

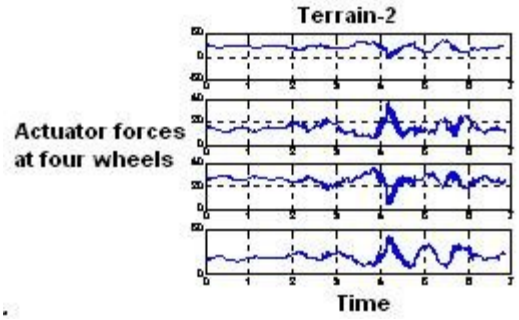

Fig. 8 The plot of actuator forces for terrain-2

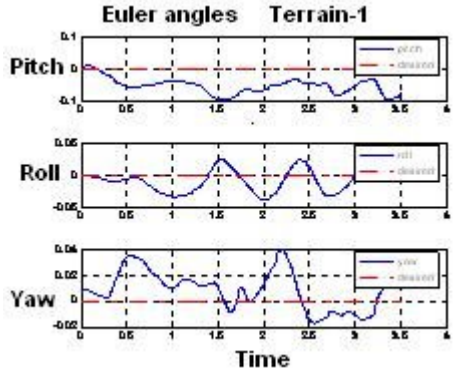

Fig 9 .Plot of Euler angles - terrain-1

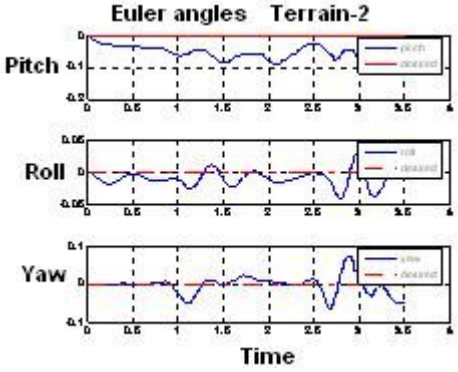

Fig10: Plot of Euler angles- terrain-2

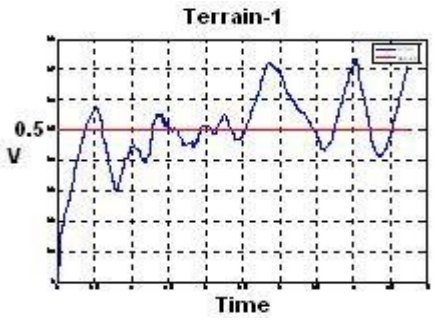

Fig.11 Plot of Velocity for terrain -1.

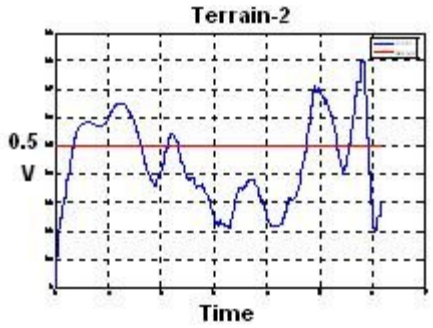

Fig.12 Plot of Velocity for terrain -2.

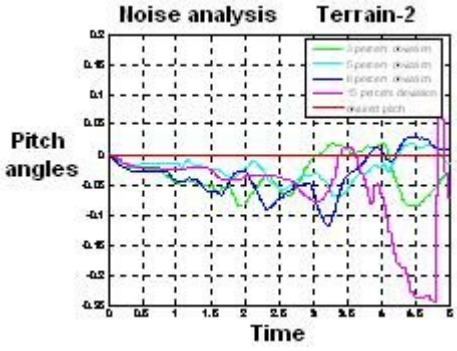

Fig. 13 Pitch Angles for noise analysis for terrain-2

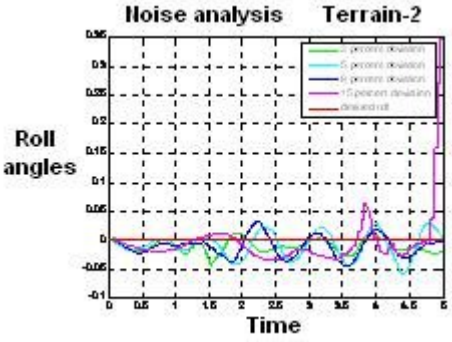

Fig. 14 Roll Angles for noise analysis for terrain-2

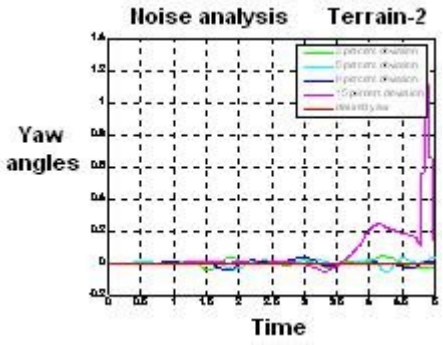

Fig. 15 Yaw Angles for noise analysis for terrain-2

Noise Analysis: Figures 13-15 show the performance of the system in presence of additive Gaussian noise at the points where contact forces are measured, whose mean is varied by 15% of the original value. The system was stable for a deviation of 15% until it encounters highly uneven terrain which is shown where the Euler angles go out of bound at the end of the simulation.

V. Conclusions and Future Work

In our work we presented a LFA-V enabling it to negotiate uneven terrain by modifying the contact forces. Such an approach for rough terrain mobility does not seem to have reported in the literature. Quasi static analysis for the system along with motivation for using LFA-V over and above a passive suspension system by depicting enhanced feasibility regions was reported. The efficacy of this method was confirmed by the plots of Euler angles which were well within the acceptable limits ensuring desired posture. From the noise analysis, stability of the system was ensured for reasonable values of sensor noise at the points where contact forces were measured. The future scope of this effort includes developing a system with a force actuated leg which has 2-DOF that can negotiate long steep slopes as well as stairways.

References

[1] T. Estier, Y. Crausaz, B. Merminod, M. Lauria, R. Piguet, and R. Siegwart, "An innovative space rover with extended climbing abilities," in *Proc. Int. Conf. Robotics in Challenging Environments*, Albuquerque, USA, 2000.

[2] R. Volpe, J. Balaram, T. Ohm and R. Ivlev, "Rocky 7: A next generation mars rover prototype," *J. Advanced Robotics*, vol. 11, no. 4, pp. 341–358, Dec. 1997.

[3] K. Iagnemma, A. Rzepniewski, S. Dubowsky and P. Schenker, "Control of robotic vehicles with actively articulated suspensions in rough terrain," *Autonomous Robots*, vol. 14, no. 1, pp. 5–16, 2003.

[4] S. V. Sreenivasan and K. J. Waldron, "Displacement analysis of an actively articulated wheeled vehicule configuration with extensions to motion planning on uneven terrain," *ASME J. Mechanical Design*, vol. 118, no. 6, pp. 312–317, 1996.

[5] CH. Grand, F. BenAmar, F. Plumet and Ph. Bidaud, "Stability and traction optimization of a reconfigurable wheel-legged robot," *Int. J. Robotics Research*, Oct. 2004.

[6] K. Iagnemma and S. Dubowsky, "Traction control of wheeled robotic vehicles in rough terrain with application to planetary rovers," *Int. J. Robotics Research*, vol. 23, no. 10-11, pp. 1029-1040, Oct.-Nov. 2004.

[7] John J. Craig, "Introduction to Robotics – Mechanics and Control," Third Edition , *Prentice Hall*.

[8] CH. Grand, F. BenAmar, F. Plumet and Ph. Bidaud, "Decoupled control of posture and trajectory of the hybrid wheel-legged robot hylos," in *Proc. IEEE Int. Conf. Robotics and Automation*, New Orleans, LA, 2004, vol. 5, pp. 5111-5116.